ISSN : 0974 - 7486 Volume 10 Issue 5

Materials Science

An Indian Journal

Full Paper

MSAIJ, 10(5), 2014 [165-172]

Thermodynamic study, elaboration and high temperature oxidation of alloys highly strengthened by tantalum carbides. Part 2: Case of a Ni-30Cr-1C-15Ta alloy

Laura Corona[1,2], Patrice Berthod[1,2,3]*

[1]University of Lorraine, B.P. 70239, 54506 Vandoeuvre-lès-Nancy – (FRANCE)

[2]Faculty of Sciences and Technologies, B.P. 70239, 54506 Vandoeuvre-lès-Nancy – (FRANCE)

[3]Institut Jean Lamour (UMR 7198), Team 206 "Surface and Interface, Chemical Reactivity of Materials", B.P. 70239, 54506 Vandoeuvre-lès-Nancy – (FRANCE)

E-mail : Patrice.Berthod@univ-lorraine.fr

ABSTRACT

In this second part of the present work dealing with chromium-rich alloys containing high amounts in carbon and tantalum, a Ni-30Cr-1C-15Ta alloy was elaborated by foundry, after preliminary thermodynamic calculations. These ones showed not the good nature of carbides but allowed anticipating a pro-eutectic solidification as carbides and not as matrix, as previously seen for the Co-30Cr-1C-15Ta cobalt alloy studied in the first part. The hardness of the obtained nickel alloy was rather high but a little lower than for the cobalt alloy one. Its behaviour in oxidation at high temperature was also good, with a chromia-forming character still subsisting even after 46 hours at 1150°C. Some interesting differences about as-cast microstructure, sub-surface microstructure evolution and of general behaviour in high temperature oxidation were noticed between this nickel alloy by comparison with the analogous cobalt alloy.

KEYWORDS

Nickel alloys;
Tantalum carbides;
Thermodynamic calculations;
Microstructures;
Hardness;
High temperature oxidation.

INTRODUCTION

Even if the aluminium-containing nickel-based alloys are maybe better known, notably as γ/γ' superalloys which feature among the best ones for high temperature applications under mechanical stresses in oxidizing atmospheres, the chromium-rich nickel-based alloys represent a high temperature alloys' family of interest. They can be still encountered in the aero-engines and hot industrial processes[1,2] (resistance against hot corrosion ensured by several tens percents of chromium) as well as in low or room temperatures applications as prosthetic dentistry[3,4] in which high mechanical properties and resistance against aqueous corrosion are required (here too favoured by chromium). Cr being a carbide-forming element the addition of carbon may lead to the development of carbides in such alloys, and with sufficient amounts of C and Cr together it is possible to obtain hard particles for achieving wear resistance[5-8].

As realized in the first part of this work with a cobalt alloy[9], the addition of a great quantity (15wt.%) of the strong carbide-former element Ta to a Ni(bal.)-30Cr-1C (all contents in wt.%) base was tested in or-

der to explore the as-cast microstructure resulting from solidification and solid state cooling in fast conditions, the level of hardness obtained for the alloy, and its behaviour in oxidation at high temperature. The final objective was here too to examine if such an alloy presents some of the required properties to candidate as a possible alternative to other carbides-hardened alloys.

EXPERIMENTAL

As for the cobalt alloy studied in the first part of this work, preliminarily thermodynamic calculations were carried out get previsions about the development of the microstructure during solidification and solid state cooling. This was here too realized by using the Thermo-Calc version N software[10], but this time with a database initially containing the descriptions of the Ni-Cr-C system and its sub-systems[11] enriched by the description of the binary and ternary sub-systems Ta-C, Ni-Ta, Cr-Ta and Ni-Ta-C[12-15]. Here too calculations were used to predict the appearance and disappearance of the successive phases, their theoretic mass fractions and chemical compositions versus temperature, from the start of solidification down 500°C, temperature at which it can be reasonably considered that additional solid state transformations have not time to occur.

The alloy considered in this second part of this work is also quaternary, and has the following targeted composition: Ni-30Cr-1C-15Ta (all contents in weight percents). It was also elaborated by foundry under 300mbars of pure Argon from pure elements (Ni, Cr and Ta: Alfa Aesar, purity higher than 99.9 wt.%; C: graphite). The same CELES high frequency induction furnace was used for achieving melting. Solidification was achieved in the water–cooled copper crucible of the HF furnace in which fusion was realized. The obtained ingot, of about forty grams, was cut to obtain a sample for the as-cast microstructure observations and the 30kg-Vickers hardness measurements (Testwell Wolpert) and another one for the exposure at 1150°C for 1150°C in a resistive tubular furnace for characterizing the high temperature oxidation behaviour of the alloy. The later one, the surface of which was preliminarily polished with 1200-grade SiC paper, was heated at +20°C min^{-1} up to the stage temperature of 1150°C at which it was maintained during 46 hours. The oxidized sample was thereafter cooled slowly in the shut-down furnace.

The as-cast sample and the oxidized sample, the later one preliminarily covered by electrolytic Ni-coating for oxide scale protection during cutting, were cut and embedded in a cold resin mixture (resin CY230 + hardener HY956). They were polished first with SiC papers from 240 to 1200 grit and second, after ultrasonic cleaning, with a textile disk enriched with 1μm alumina particles. These metallographic samples were observed using a Scanning Electron Microscopy (SEM JEOL JSM-6010LA), in the Back Scattered Electrons mode (BSE) under an acceleration voltage of 20kV. The bulk microstructure of the as-cast alloy as well as the oxide scale and alloy sub-surface for the sample exposed to high temperature, were characterized.

RESULTS AND DISCUSSION

Thermodynamic calculations

The evolutions of the mass fractions when temperature decreases are graphically presented in Figure 1, by assuming that solidification and solid state cooling can be described by the successive equilibria computed by Thermo-Calc. The liquid phase logically stays at 100% of mass fraction (Figure 1) and keeps its chemical composition Ni-30Cr-1C-15Ta (Figure 2) until the appearance of a new second phase. This occurs at 1375.26°C, temperature at which the first solid forms: the M_7C_3 chromium carbides. During the loss of about one hundred of Celsius degrees the $M_{23}C_3$ carbides grows alone in the liquid, up to 5.50 mass.% at 1272.52°C temperature at which a second solid phase appears too: the FCC nickel-based matrix. This is a first eutectic part of the end of solidification during which the M_7C_3 and FCC Ni matrix mass fractions increase up to 9.41 mass.% and 53.34 mass.% respectively. Under 1241.67°C, temperature at which a second form of chromium carbides appears, $M_{23}C_6$, the M_7C_3 mass fraction decreases and disappears when reaching 1170.31°C while the $M_{23}C_6$ phase now represents 17.4 mass.% in the alloy. Thereafter its mass fraction do not continue to evaluate since it increases only up to 17.61 mass.% at 500°C. Before the disappearance of the M_7C_3 solidification reached its end at 1235.28°C, with for the alloy a metallurgical state composed of 81.74

mass.% of FCC Ni matrix, 17.4 mass.% of $M_{23}C_6$ and also 2.15 mass.% of a first intermetallic compound involving nickel and tantalum Ni_3Ta.

Finally, after cooling down to 500°C, the theoretical microstructure of the alloy is composed of 49.32% of matrix, 17.61 % of $M_{23}C_6$ carbides, 24.88% of Ni_3Ta and 8.19% of a second intermetallic compound, Ni_8Ta, appeared at 645.48°C (all fractions in mass percentage).

The chemical compositions of the different phases from their appearance to their eventual disappearance before 500°C are graphically represented in Figure 2 for the liquid phase, Figure 3 for the M_7C_3 carbide, Figure 4 for the $M_{23}C_6$ carbide, Figure 5 for the FCC Ni matrix, Figure 6 for the first intermetallic compound to appear (Ni_3Ta) and Figure 7 for the second one (Ni_8Ta).

From the start of solidification the liquid losses chromium and carbon, consequently to the pro-eutectic M_7C_3 precipitation (phenomena accelerating when the $M_{23}C_6$ carbides appear), while its tantalum content remains stable until the start of matrix solidification. When this occurs, the nickel content starts decreasing while the tantalum content in liquid increases to reach more than 22 mass.% after only a cooling of slightly less than

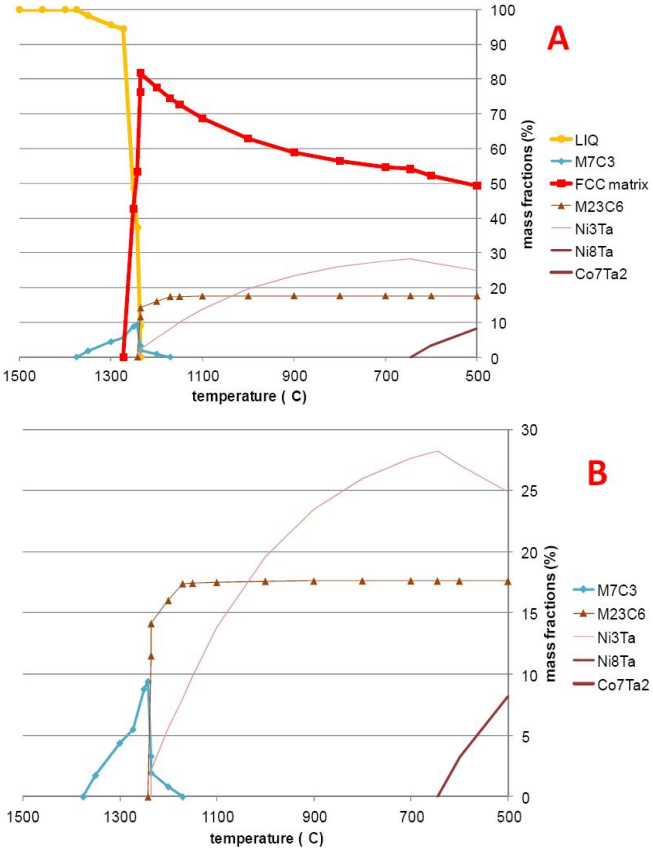

Figure 1 : Development of the microstructure of the Ni-30Cr-1C-15Ta alloy during solidification, according to Thermo-Calc (B : enlargement of the low mass fractions part of A)

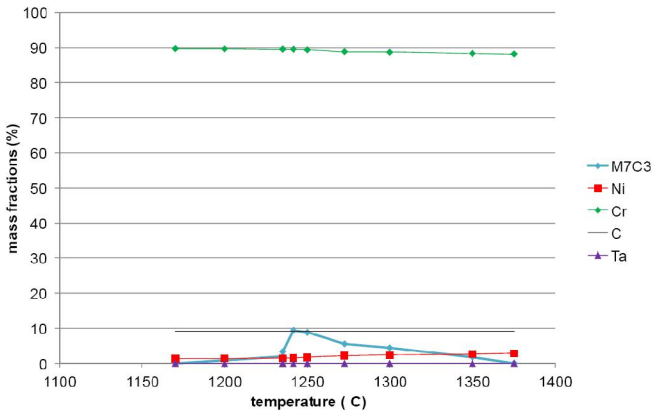

Figure 3 : Evolution of the mass fraction and of the chemical composition of the M_7C_3 phase during the cooling until its disappearance (according to Thermo-Calc)

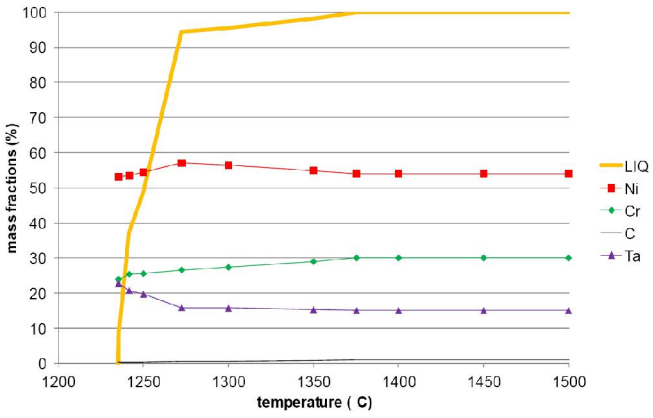

Figure 2 : Evolution of the mass fraction and of the chemical composition of the liquid phase during the cooling until its disappearance (according to Thermo-Calc)

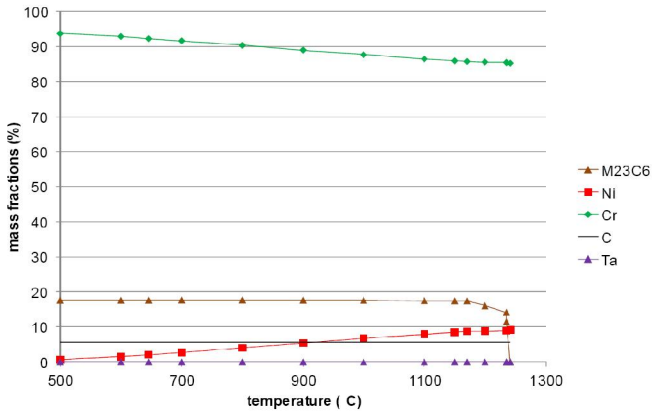

Figure 4 : Evolution of the mass fraction and of the chemical composition of the $M_{23}C_6$ phase during the cooling down to 500°C (according to Thermo-Calc)

Full Paper

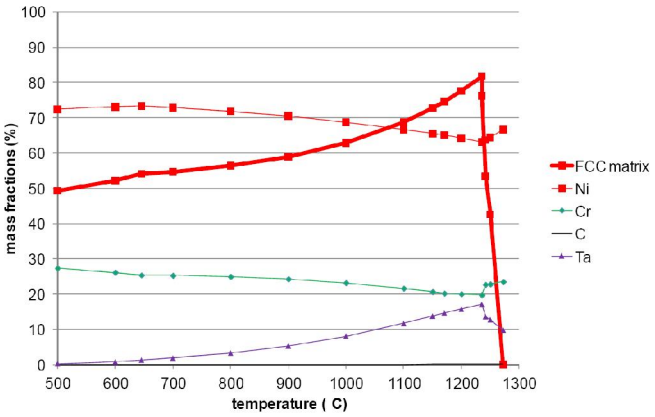

Figure 5 : Evolution of the mass fraction and of the chemical composition of the FCC matrix phase during the cooling down to its disappearance (according to Thermo-Calc)

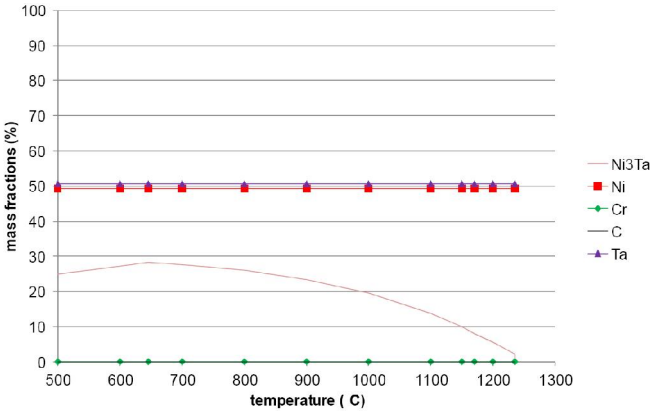

Figure 6 : Evolution of the mass fraction and of the chemical composition of the Ni_3Ta intermetallic compound during its short existence (according to Thermo-Calc)

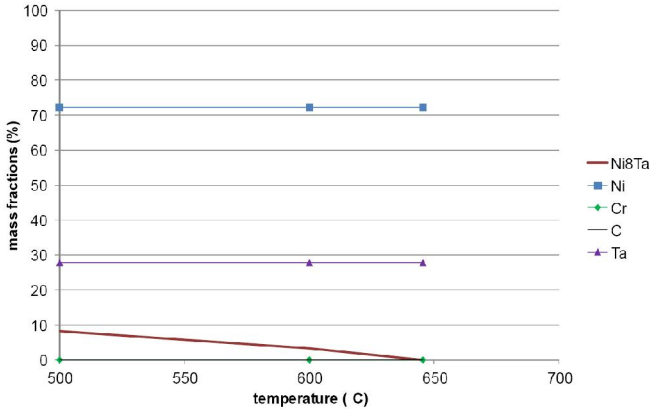

Figure 7 : Evolution of the mass fraction and of the chemical composition of the Ni_8Ta intermetallic compound during its short existence (according to Thermo-Calc)

40°C only. This involves a Ta segregation in the last zones to solidify.

The chemical compositions of the two types of carbides also change during the cooling, with a small progressive replacement of nickel (minor element in these phases) by chromium (major element).

During the cooling down to 500°C, the contents in Ta and in Cr in the matrix start to respectively increase and decrease, and these tendencies become inversed near 1235°C. The Ta content continuously decreases with the growth of the tantalum-rich intermetallic compounds and the Cr content increases only because of the decrease of the matrix mass fraction for a given Cr quantity.

Concerning the two intermetallic compounds there are logically no dependence on temperature for their chemical compositions, this being due to their stoichiometric character.

The obtained as-cast microstructure

A micrograph illustrating the as-cast microstructure of this Ni-30Cr-1C-15Ta studied alloy after its solidification and its cooling down to room temperature is given in Figure 8, together with the global chemical composition (EDS measurement in the centre of the ingot).

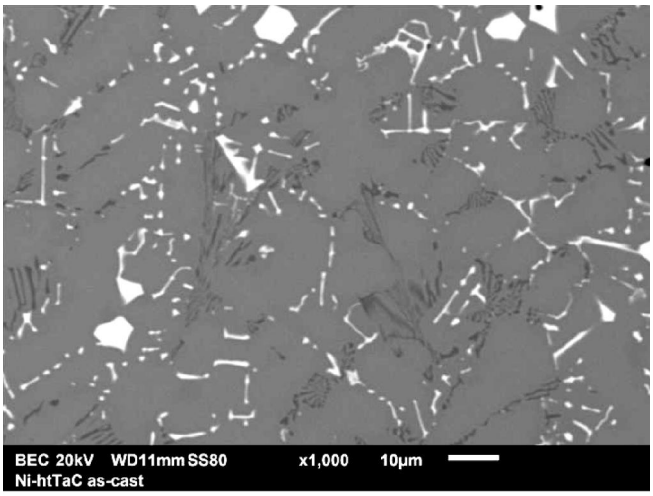

General composition: 55.66Ni-32.11Cr-12.23Ta+C (wt.%)

Figure 8 : The as-cast microstructure of the Ni-30Cr-1C-15Ta and the obtained general chemical composition of the alloy (SEM/BSE micrograph)

The centre of the Ni-30Cr-1C-15Ta ingot presents a microstructure which is composed of a dendritic matrix of cobalt solid solution, of white particles – some of them script-like and situated in the interdendritic spaces and the other ones more compact – and elongated acicular particles mixed with matrix and darker than it. It can be noted that the later type of particle was not present in the analogous alloy but based on cobalt which

was examined in the first part of this work[9]. The global chemical composition is not far from the targeted one but it can be noticed a tantalum content sensibly lower than wished, as for the similar cobalt-based alloy[9]. In contrast carbon remains not known since the EDS technique is not able to correctly determine the content in a so light element.

EDS pinpoint measurements were carried out in the matrix and in the white compact particles. It was not possible to do that on the script-like and acicular white and dark particles since their thicknesses were too low. The obtained results show that the tantalum content in matrix is rather high (about 5.7 wt.%Ta) which is significantly higher than determined in the matrix of the similar cobalt-based alloy (about 3.3 wt.%Ta). The white compact particles are clearly TaC carbides and one can guess that the script-like one are TaC too since their white level is the same.

The microstructure is not homogeneous since, as already encountered for the similar cobalt-based alloy[9] the most external part of the ingot is particularly rich in TaC carbides (Figure 10).

Three Vickers indentations were carried out under a load of 30kg in the centre of the ingot. The values presented in TABLE 1 show that the average hardness obtained is rather high for a nickel-based alloy but a little lower than obtained in the similar cobalt alloy (about 435 Hv_{30kg}).

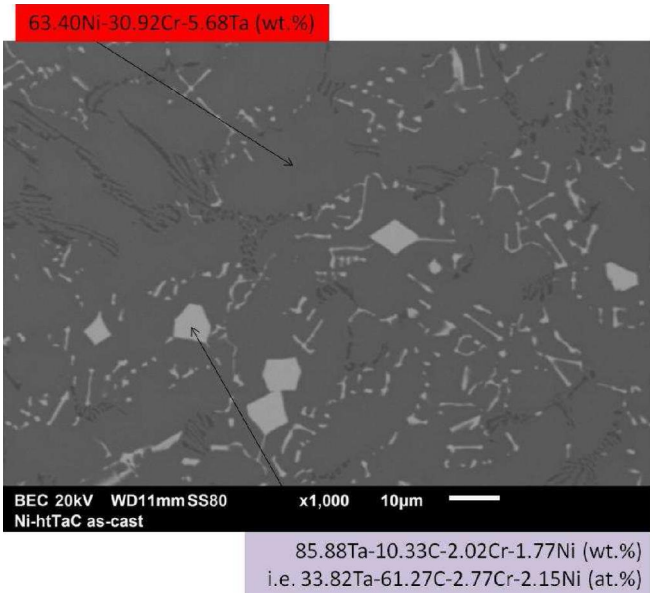

Figure 9 : Some results of matrix chemical composition and of particles identification (SEM/EDS measurements)

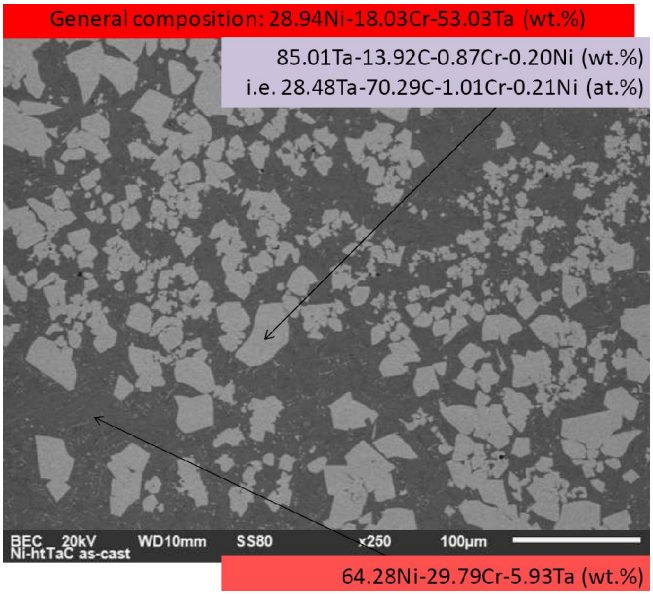

Figure 10 : Aspect of the external part of the ingot and pinpoint chemical analysis of this special zone (SEM/BSE and SEM/EDS measurements)

TABLE 1 : Results of Vickers indentations on the as-cast alloy (load : 30 kg)

Individual values	Average hardness	Standard deviation
283-301-294	293	9

Behaviour in high temperature oxidation

The sample exposed to the laboratory air during 46 hours at 1150°C in the tubular furnace (cut in the centre of the initial ingot) was also metallographically examined concerning its surface state. This one is illustrated by the SEM/BSE micrograph presented in Figure 11. It appears that an external oxide was covering the whole surface when the sample was at high temperature. Unfortunately, as already encountered for the cobalt version[9], the main part of this oxide was lost during the cooling, except some rare parts being still available for further characterization. Here too internal oxidation occurred in the subsurface, leading to the appearance of a population of pale oxides in the most external part of the carbide-free zone. One can notice that the average depth of this carbide-free zone, which is of about 70µm, is twice the one measured for the cobalt alloy[9]. Another difference by comparison with the cobalt alloy is the obvious modification of the carbides characteristics in a more internal zone (thickness of 150-200µm) separating the carbide-free zone and the bulk: here carbides seems being more present in

Full Paper

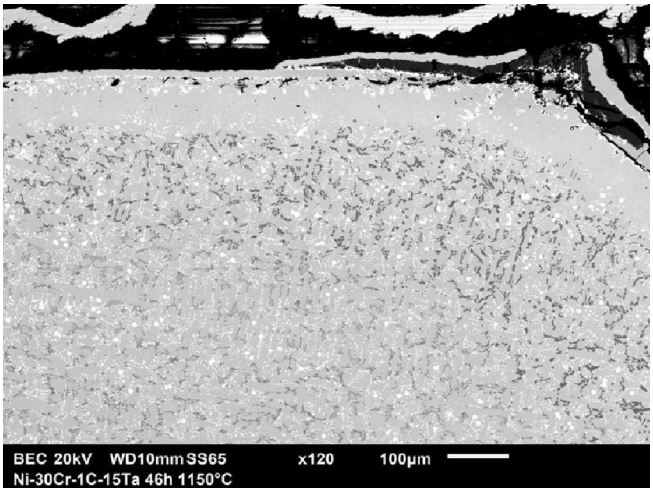

Figure 11 : General aspect of the external surface of the sample after exposure to laboratory air at 1150°C during 46 hours (SEM/BSE micrograph)

term of surface fraction and the proportion of chromium carbides is higher than deeper (and maybe the proportion of tantalum carbide is lower than deeper).

EDS pinpoint chemical data were acquired on the different types of oxides (Figure 12). As evidenced in TABLE 2, the dark oxide formed all around the sample (and for which only some parts are still present after cooling and the resulting oxide desquamation) is chromia. The white oxide present as isolated particles in the most external part of the carbide-free zone (but in quantities lower than for the cobalt alloy[9]) as well as the continuous layer of white oxide detached with chromia from the alloy before (or during) the electrolytic Ni deposition (EDS point '004' in Figure 12), are the $CrTaO_4$ oxide.

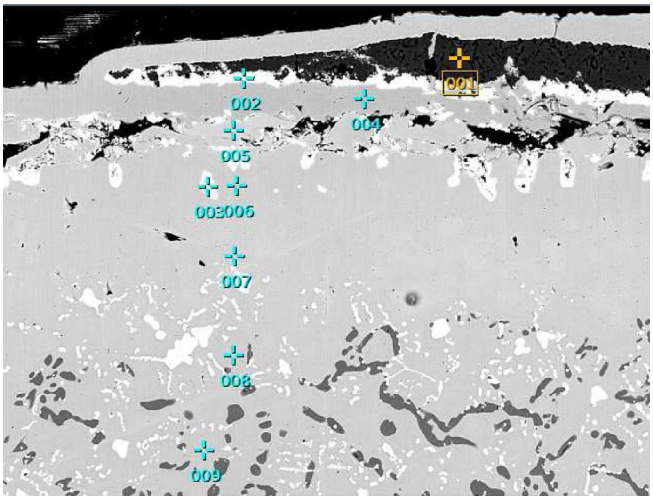

Figure 12 : Locations of the EDS measurements (EDS/BSE micrograph)

TABLE 2 : Chemical composition of the two types of oxides formed on surface and in the subsurface; locations numbered according to Figure 12

Oxides' compositions in at.% (and wt.%)	O	Cr	Ta	Ni
001 (→ Cr_2O_3)	63.10 at.% (34.32 wt.%)	36.45 at.% (64.43 wt.%)	0.08 at.% (0.51 wt.%)	0.37 at.% (0.74 wt.%)
002 (→ $CrTaO_4$ + partly electrolytic Ni, 004 : Ni > 99%)	32.55 at.% (8.84 wt.%)	10.79 at.% (9.53 wt.%)	12.13 at.% (37.25 wt.%)	44.53 at.% (44.38 wt.%)
003 (→ $CrTaO_4$ + partly matrix)	56.90 at.% (15.37 wt.%)	16.69 at.% (14.66 wt.%)	21.21 at.% (64.81 wt.%)	5.20 at.% (5.16 wt.%)

The results of the series of EDS pinpoints measurements acquired in the sub-surface at an increasing depth from the oxide/alloy interface (locations visible in Figure 12 too) are displayed in TABLE 3. These values show that the Cr-deleted zone is 300-400µm deep with a minimal content on extreme surface equal to 23 wt.%, which is still a rather high value for an 30wt.%Cr-containing alloy exposed during almost fifty hours at such high temperature. The content in tantalum is curiously slightly higher in the carbide-free zone than in in the matrix of the zone still containing carbides, possible consequence of the disappearance of tantalum carbides.

TABLE 3 : Evolution of the local chemical composition with the depth from extreme surface (EDS pinpoint analysis); locations numbered according to Figure 12

005	006	007	008	009	Element (wt.%)
23.15	23.53	24.84	27.24	28.08	Cr
7.21	6.07	7.06	5.83	5.35	Ta
69.64	70.40	68.10	66.93	66.57	Ni

General commentaries

As for the cobalt alloy studied in the first part of this work it appeared here that carbon and tantalum contents increased up to 1wt.% C and 15 wt.% Ta leads to more carbides, a significant part of them having migrated to the external part of the liquid ingot (only pro-eutectic TaC formed before matrix solidification start). There is however great differences with what was

seen for the cobalt alloy, for the thermodynamic calculations (theoretically mainly TaC carbides for the cobalt alloy and Ta-rich intermetallics instead TaC and exclusively chromium carbides of two types for the nickel alloy), and for the microstructures really obtained (only TaC in the cobalt alloy and TaC with chromium carbides in the nickel alloy). The microstructures obtained in the real alloy here are in great disagreement with what the thermodynamic calculations predicted. Indeed a significant part of tantalum carbides exists in this nickel alloy, besides the numerous chromium carbides, and the pro-eutectic carbides which formed at the early stages of solidification (and thereafter found partly in the solidified ingot center and partly in the solidified ingot periphery) were obviously tantalum carbides and not chromium carbides as suggested by the thermodynamic calculations. Such mismatches between calculations and real experience were already earlier found for chromium-rich nickel-based alloys with 0.2 to 0.4%C and 3 to 6%Ta (weight contents)[16], for the same database used for the thermodynamic calculations, this showing that this thermodynamic database needs to be improved.

Nevertheless, despite such mismatches, the preliminary thermodynamic calculations demonstrated that solidification started with a carbide precipitation, with consequently a migration of blocky carbides towards the periphery, as earlier encountered for nickel alloys very rich in chromium carbides[17] and more recently with nickel alloys containing hafnium carbides[18]. Despite this partly loss of carbides the hardness, remains about 100 Hv30kg-higher than the one of Ni-30Cr-xC alloys with the same carbon content (x=1wt.%)[19].

Concerning the oxidation results of the exposures to high temperature, which were realized during the same rather long time (46 hours) and the same high temperature (1150°C) as for the cobalt alloy of the first part[9], no severe surface degradation was noticed. The parts of external oxides remained on surface and then analyzed showed that the alloy was still chromia-forming, while there was no real microstructure degradation (except the partly nature change just deeper than the carbide-free zone). One can additionally notice the lower amount of internal $CrTaO_4$ oxide in the thin subsurface by comparison with the cobalt alloy[9].

CONCLUSIONS

Here too, the high contents in carbon and in tantalum led to a dense population of carbides, but composed of both tantalum carbides and chromium carbides. Their interdendritic repartition as well as their script-like or acicular forms and mixing with matrix, may favour good mechanical behaviour at medium and high temperatures. The room temperature hardness is rather high but a little lower than for the cobalt alloy studied in the first part. The high temperature oxidation resistance is, for this nickel-based alloy too, very good and the chromium content maintained high (more than 20 wt.%) in extreme surface may allow the alloy keeping its chromia-forming behaviour a long additional time.

REFERENCES

[1] M.A.Engelman, C.Blechner; The New York Journal of Dentistry, **46**, 232 **(1976)**.
[2] E.F.Huget, N.Dvivedi, H.E.Cosner; The Journal of the American Dental Association, **94**, 87 **(1977)**.
[3] C.T.Sims, W.C.Hagel; The superalloys, John Wiley & Sons, New York, **(1972)**.
[4] M.J.Donachie, S.J.Donachie; Superalloys: A Technical Guide, 2nd Edition, ASM International, Materials Park, **(2002)**.
[5] A.Klimpel, L.A.Dobrzanski, A.Lisiecki, D.Janicki; Journal of Materials Processing Technology, **164-165**, 1068 **(2005)**.
[6] Z.T.Wang, H.H.Chen; Mocaxue Xuebao Tribology, **25**, 203 **(2005)**.
[7] H.Han, S.Baba, H.Kitagawa, S.A.Suilik, K.Hasezaki, T.Kato, K.Arakawa, Y.Noda; Vacuum, **78**, 27 **(2005)**.
[8] D.Zhang, X.Zhang; Surface and Coating Technology, **190**, 212 **(2005)**.
[9] L.Corona, P.Berthod; Materials Science: An Indian Journal, submitted.
[10] Thermo-Calc version N; Foundation for Computational Thermodynamics, Stockholm, Sweden, Copyright, **(1993,2000)**.
[11] SGTE; Scientific Group Thermodata Europe database, update, http://www.SGTE.org., **(1992)**.
[12] K.Frisk, A.F.Guillermet; Journal of Alloys and Compounds, **238**, 167 **(1996)**.
[13] I.Ansara, M.Selleby; Calphad, **18**, 99 **(1994)**.
[14] N.Dupin, I.Ansara; Journal of Phase Equilibria, **14**,

451 **(1993)**.
[15] N.Dupin, I.Ansara; Zeitschrift für Metallkunde, **87**, 555 **(1996)**.
[16] P.Berthod, L.Aranda, C.Vébert, S.Michon; Calphad, **28**, 159 (2004).
[17] P.Berthod, E.Souaillat, O.Hestin; Materials Science: An Indian Journal, **6(4)**, 260 **(2010)**.
[18] P.Berthod; Materials Science: An Indian Journal, **9(9)**, 359 **(2013)**.